



ORIGINAL ARTICLE

# Visible light induced degradation of methyl orange using $\beta$ - $\text{Ag}_{0.333}\text{V}_2\text{O}_5$ nanorod catalysts by facile thermal decomposition method



R. Saravanan <sup>a,e,\*</sup>, Vinod Kumar Gupta <sup>b,c,d</sup>, Edgar Mosquera <sup>e</sup>, F. Gracia <sup>a</sup>,  
V. Narayanan <sup>f</sup>, A. Stephen <sup>g,\*</sup>

<sup>a</sup> Department of Chemical Engineering and Biotechnology, University of Chile, Beauchef 850, Santiago, Chile

<sup>b</sup> Department of Chemistry, Indian Institute of Technology Roorkee, Roorkee 247 667, India

<sup>c</sup> Center for Environment and Water, The Research Institute, King Fahd University of Petroleum and Minerals Dhahran, Saudi, Saudi Arabia

<sup>d</sup> Department of Applied Chemistry, University of Johannesburg, Johannesburg, South Africa

<sup>e</sup> Nanoscale Materials Laboratory, Department of Materials Science, University of Chile, Avenida Tupper 2069, Santiago, Chile

<sup>f</sup> Department of Inorganic Chemistry, University of Madras, Guindy Campus, Chennai 600 025, India

<sup>g</sup> Department of Nuclear Physics, University of Madras, Guindy Campus, Chennai 600 025, India

Received 27 February 2015; accepted 6 June 2015

Available online 16 June 2015

## KEYWORDS

Thermal decomposition method;  
Nanorods;  
Degradation;  
Photocatalytic activity

**Abstract** One dimensional nanorods of  $\beta$ - $\text{Ag}_{0.333}\text{V}_2\text{O}_5$  have been synthesized by facile thermal decomposition method without using any additives. The prepared sample was characterized by different physical and chemical techniques such as XRD, FE-SEM, TEM, DRS and XPS. The photocatalytic activity of  $\beta$ - $\text{Ag}_{0.333}\text{V}_2\text{O}_5$  catalyst was investigated by studying the degradation of methyl orange (MO) in aqueous medium under visible light exposure. The result shows  $\beta$ - $\text{Ag}_{0.333}\text{V}_2\text{O}_5$  exhibits outstanding photocatalytic activity under visible light illumination.

© 2015 The Authors. Production and hosting by Elsevier B.V. on behalf of King Saud University. This is an open access article under the CC BY-NC-ND license (<http://creativecommons.org/licenses/by-nc-nd/4.0/>).

\* Corresponding authors at: Department of Chemical Engineering and Biotechnology, Universidad de Chile, Av. Tupper 2007, 6th floor, Santiago 8370451, Chile. Tel.: +56 2 978 4284; fax: +56 2 699 1084 (R. Saravanan), Department of Nuclear Physics, University of Madras, Guindy Campus, Chennai-600 025, India (A. Stephen). E-mail addresses: [saravanan3.raj@gmail.com](mailto:saravanan3.raj@gmail.com) (R. Saravanan), [stephen\\_arum@hotmail.com](mailto:stephen_arum@hotmail.com) (A. Stephen).  
Peer review under responsibility of King Saud University.



Production and hosting by Elsevier

## 1. Introduction

In the last few decades, across global environmental focusing, numerous conventional methods have been proposed to resolve the aquatic contaminants being faced by all living things in this world [1]. Nevertheless, each method has its shortcomings. Advanced oxidation processes have become of widespread interest in research and development of waste water treatment technologies. Among the advanced oxidation processes, photocatalysis is one of the potential and constructive avenues to the mineralization of organic pollutants,

including organic dyes due to its low cost, complete mineralization, no other secondary pollutions and only mild temperature necessity [2–5]. Titanium oxide (TiO<sub>2</sub>) and zinc oxide (ZnO) have been extensively used as photocatalysts due to their low cost, chemical stability against photocorrosion and chemical corrosion [6–8]. However, their relative bandgap diminishes their applications in the visible region of the solar spectrum. Thus, significant efforts have been directed toward the research on suitable visible light driven catalysts. In particular, silver vanadium oxide (SVO) has been an excellent visible light responsive catalyst due to its smaller bandgap, chemical and thermal stability allows to exploit it as an attractive material for diverse applications such as cathode active material in lithium ion batteries, photocatalysts and antibacterial activity [9–11].

It is well known that the properties of nanostructured materials depend on the shape and size or the morphology of these materials. One-dimensional nanostructures (1D) have great advantageous features over the bulk and other nanostructured materials like 2d due to their unique and fascinating properties such as the high surface to volume ratio, dimensionality and small size [12]. Therefore, extensive efforts have been focused on fabricating various nanostructures of SVO such as nanobelts, nanowires, nanoribbons, nanotubes, nanorods by various methods [13–14]. However, it remains a great challenge to develop low cost facile synthetic route.

In this report, 1D nanorods of  $\beta$ -Ag<sub>0.333</sub>V<sub>2</sub>O<sub>5</sub> were successfully synthesized by novel thermal decomposition method. The prepared sample was characterized by various techniques and their results are discussed in detail. Furthermore, the photodecomposition of methyl orange (MO) in the presence of  $\beta$ -Ag<sub>0.333</sub>V<sub>2</sub>O<sub>5</sub> was investigated under visible light irradiation and results are discussed in detail.

## 2. Experimental procedure

### 2.1. Materials

Ammonium meta vanadate (Sigma–Aldrich) and silver acetate (Rankem) used in the present study are of analytical reagent grade. Methyl orange (MO) dyes were purchased from Sigma–Aldrich chemicals. All the chemicals were used as received without further purification. All aqueous solutions were prepared using double distilled water.

### 2.2. Catalyst preparation

The  $\beta$ -Ag<sub>0.333</sub>V<sub>2</sub>O<sub>5</sub> catalyst preparation is based on thermal decomposition of ammonia and acetate group under high temperature condition without the presence of any additive [15–16]. 0.578 g of ammonium meta vanadate and 0.154 g of silver acetate were measured, they were mixed and ground well for 3 h in a mortar. Later it was calcined at 400 °C for 3 h in a muffle furnace using an alumina crucible. The decomposition temperature was obtained from the phase diagram reported in the reference [9]. During the calcination, the temperature was raised at a speed of 4 °C/min and after the heat treatment, the sample was cooled to room temperature naturally.

### 2.3. Characterization

The structure of the material was identified by Rich Siefert 3000 X-ray diffractometer using Cu K<sub>α1</sub> radiation with  $\lambda = 1.5406$  Å. Surface morphology, elemental analysis and energy dispersive X-ray spectroscopy (EDS) analysis were carried out using field emission scanning electron microscope (FE-SEM, HITACHI-SU6600). TEM analysis was carried out using JEOL 2000FX microscope operated at 200 kV. UV–Vis diffuse reflectance spectrum was measured by CARY 5E UV–VIS–NIR spectrophotometer. Chemical states of catalysts were examined by using DRA 400 – XM1000 OMICRON X-ray photoelectron spectroscopy. The photocatalytic activity was measured by a UV–Visible spectrophotometer (Perkin Elmer Lambda 11, USA).

### 2.4. Photocatalytic activity measurement

Photocatalytic effect of  $\beta$ -Ag<sub>0.333</sub>V<sub>2</sub>O<sub>5</sub> nanorods was investigated by the photodegradation of MO chosen as a model organic dye under visible light irradiation. A solution of MO dyes with the initial concentration of  $3 \times 10^{-5}$  mol/L was prepared afresh and used. Before visible light illumination, the suspension containing 500 mg of prepared catalysts and 500 mL of MO aqueous solution was magnetically stirred for 30 min in a dark condition to ensure the adsorption equilibrium of MO on the sample surface. After that, the suspension was irradiated under visible light (7748XHP 250 W, Philips, 532 nm) which was kept under continuous stirring at room temperature to obtain full suspension of the particles throughout the experiment. During irradiation, the suspension was syringed at regular intervals of time and immediately centrifuged to wipe out the catalyst particles and then the absorbance of MO aqueous solutions was measured by UV–Vis spectrophotometer. Degradation efficiency ( $\eta$ ) can be calculated using the following equation.

$$\eta = \left[ 1 - \frac{C}{C_0} \right] \times 100 \quad (1)$$

where,  $C_0$  and  $C$  are the concentrations of the solution before illumination ( $t = 0$ ) and after illumination of light for  $t$  minutes respectively.

## 3. Results and discussions

The preparation mechanism of  $\beta$ -Ag<sub>0.333</sub>V<sub>2</sub>O<sub>5</sub> nanorods is shown in Fig. 1 and the mechanism is similar to vapor to solid mechanism [17]. The high temperature generated oxide vapor from raw material settled or deposited when the temperature was lowered. Pan et al. reported that surface defects or dislocations of the substrate provide promising nucleation sites for the oxide vapor, similarly in the present work the crucible provides such nucleation sites. The vapor condenses on these sites, forming seeds for a continuous deposition of oxide vapor [17].

The structure and crystallite size of the prepared sample were identified by XRD pattern as depicted in Fig. 2. This XRD pattern was well consistent with the standard JCPDS card no: 81-1740. All the observed diffracted peaks in this XRD pattern were indexed to monoclinic structure of  $\beta$ -Ag<sub>0.333</sub>V<sub>2</sub>O<sub>5</sub> with lattice parameters  $a = 15.34(2)$  Å,

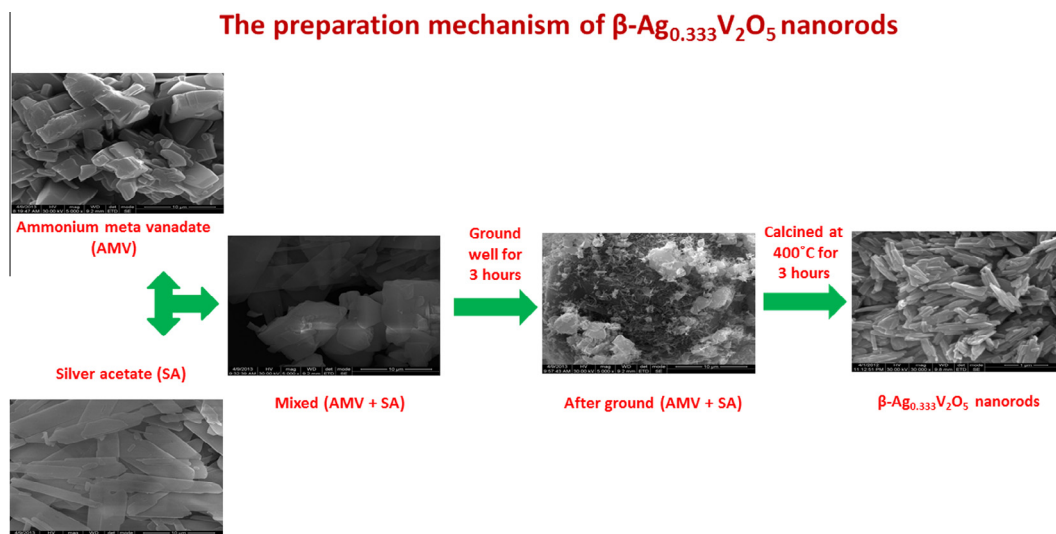


**Figure 1** Preparation mechanism of  $\beta\text{-Ag}_{0.333}\text{V}_2\text{O}_5$  nanorods.

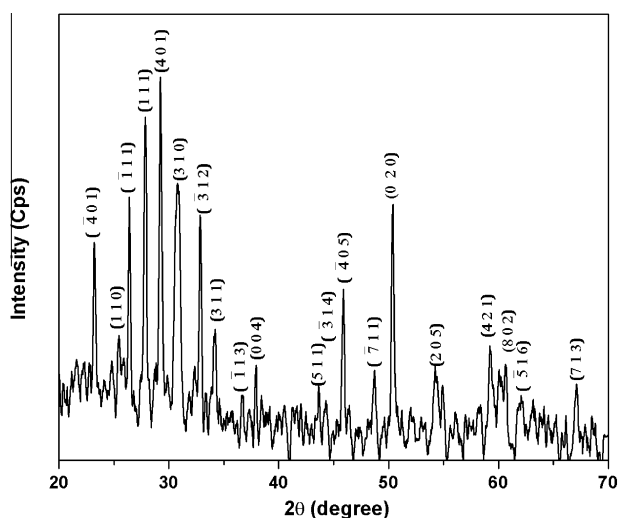


**Figure 2** XRD pattern of  $\beta\text{-Ag}_{0.333}\text{V}_2\text{O}_5$  nanorods.

$b = 3.602(5) \text{ \AA}$ ,  $c = 10.08(2) \text{ \AA}$ . The crystallite size was determined to be  $\sim 34 \text{ nm}$  from the broadening of (401) plane by using Scherrer formula [6]. Hence, this result indicates the formation of monoclinic structure of  $\beta\text{-Ag}_{0.333}\text{V}_2\text{O}_5$  and the crystallite size of the prepared sample in nanoscale range.

The surface morphology of the  $\beta\text{-Ag}_{0.333}\text{V}_2\text{O}_5$  catalyst was observed by field emission scanning electron microscope (FE-SEM). Fig. 3 shows the surface morphology of  $\beta\text{-Ag}_{0.333}\text{V}_2\text{O}_5$  catalyst. The FE-SEM image reveals that the  $\beta\text{-Ag}_{0.333}\text{V}_2\text{O}_5$  samples exhibit randomly distributed agglomerated 1D nanorods. Particle size distribution curve of the  $\beta\text{-Ag}_{0.333}\text{V}_2\text{O}_5$  catalyst was measured from FE-SEM image represented in Fig. 4 which shows  $\beta\text{-Ag}_{0.333}\text{V}_2\text{O}_5$  nanorods have an average diameter in the range of  $\sim 90 \text{ nm}$ .

The size and shape of the  $\beta\text{-Ag}_{0.333}\text{V}_2\text{O}_5$  catalyst were characterized by transmission electron microscope (TEM). The TEM image of  $\beta\text{-Ag}_{0.333}\text{V}_2\text{O}_5$  is displayed in Fig. 5(a and b). The low magnification image shows the bunch of agglomerated rod shaped nano particles. A single nanorod obtained

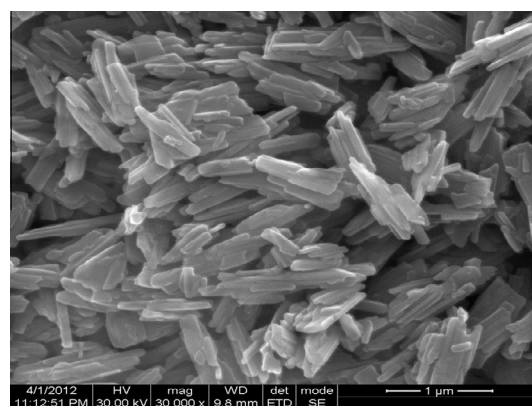


**Figure 3** FE-SEM image of  $\beta\text{-Ag}_{0.333}\text{V}_2\text{O}_5$  nanorods.

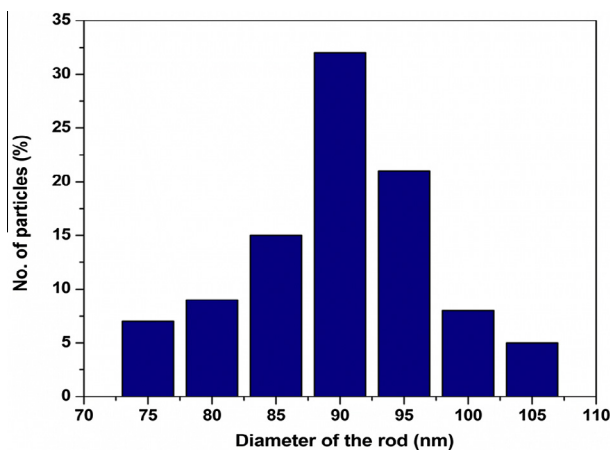


**Figure 4** Particle size distribution curve of  $\beta\text{-Ag}_{0.333}\text{V}_2\text{O}_5$  nanorods.

at high magnification is given in Fig. 5(b). According to this figure, the diameter and length of the single rod are  $\sim 90 \text{ nm}$  and  $350 \text{ nm}$  respectively. This result is in good agreement with

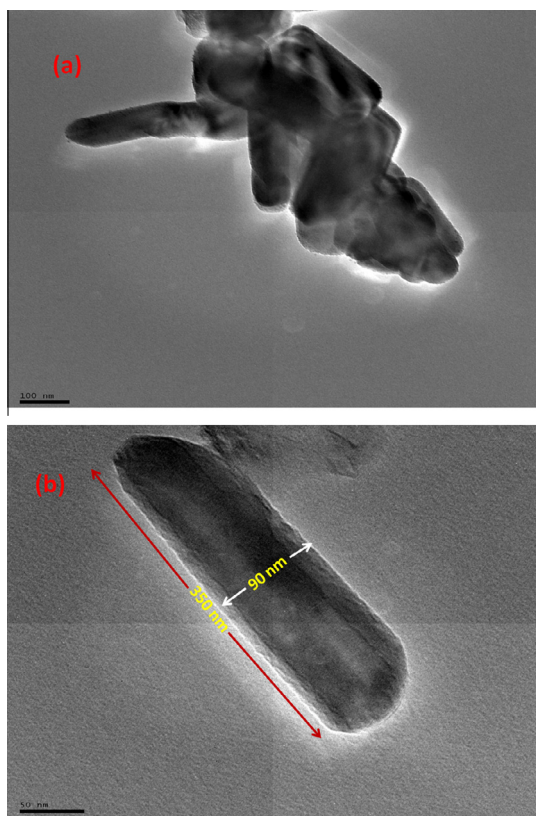


**Figure 5** TEM image of  $\beta\text{-Ag}_{0.333}\text{V}_2\text{O}_5$  nanorods (a) low magnification image and (b) high magnification image.

FE-SEM observation. Further, the presence of elements in  $\beta\text{-Ag}_{0.333}\text{V}_2\text{O}_5$  nanorods was analyzed by energy dispersive X-ray spectroscopy (EDS) and the obtained spectrum is shown in Fig. 6. From this spectrum, it is observed that the prepared

$\text{Ag}_{0.333}\text{V}_2\text{O}_5$  sample consists of vanadium (V), silver (Ag) and oxygen (O) without the existence of any other impurities. From FE-SEM, TEM and EDS results, it is concluded that the prepared  $\text{Ag}_{0.333}\text{V}_2\text{O}_5$  catalyst has a rod-like morphology without any impurities.

The room temperature UV-Vis diffuse reflectance spectrum (UV-Vis DRS) was used to examine the optical property of  $\beta\text{-Ag}_{0.333}\text{V}_2\text{O}_5$  nanorods. The bandgap value of the prepared sample was determined from the Kubelka-Munk (KM) relation [18]. Based on the equation,  $(F(R) * E)^{1/2}$  vs. photon energy ( $E$ ). The obtained bandgap energy of  $\beta\text{-Ag}_{0.333}\text{V}_2\text{O}_5$  catalysts was  $\sim 2.3$  eV which is comparable with the value reported in the literature [10–11]. The Fig. 7 represents the diffuse reflectance spectrum (UV-Vis DRS) of  $\beta\text{-Ag}_{0.333}\text{V}_2\text{O}_5$  nanorods. As seen from the inset figure, the strong absorption edge is exhibited in the red region. This result suggested that  $\beta\text{-Ag}_{0.333}\text{V}_2\text{O}_5$  sample could be used as visible light responsive catalysts for photocatalytic applications.

The oxidation states and chemical composition of the sample were examined by XPS analysis. In the XPS spectra, binding energies of the sample were calibrated by binding energy of C 1s (284.6 eV) as a reference. The obtained XPS patterns of  $\text{Ag}_{0.333}\text{V}_2\text{O}_5$  catalysts are provided in Fig. 8(a–c). The survey spectrum (Fig. 8(a)) indicates that the sample contains V, Ag and O without any other impurities except C 1s peak which comes from pump oil in the vacuum system of XPS instrument itself. Fig. 8(b) shows the binding energy of core level V(2p<sub>3/2</sub>) and V(2p<sub>1/2</sub>) located at 517.4 eV and 524.9 eV respectively which corresponds to V<sup>5+</sup> state of vanadium [19]. Mean while, the peak positioned at 530.2 eV is attributed to O 1s of V<sub>2</sub>O<sub>5</sub>, whereas the other peak at 532.4 eV is due to the OH group on the sample surface [20]. The high resolution spectrum in Fig. 8(c) shows the binding energies of Ag region at 367.5 eV and 373.5 eV are assigned to Ag(3d<sub>5/2</sub>) and Ag(3d<sub>3/2</sub>) respectively which are in good agreement with the values reported in the reference [21]. XPS profile demonstrates that Ag, V and O were present in the  $\beta\text{-Ag}_{0.333}\text{V}_2\text{O}_5$  nanorods.

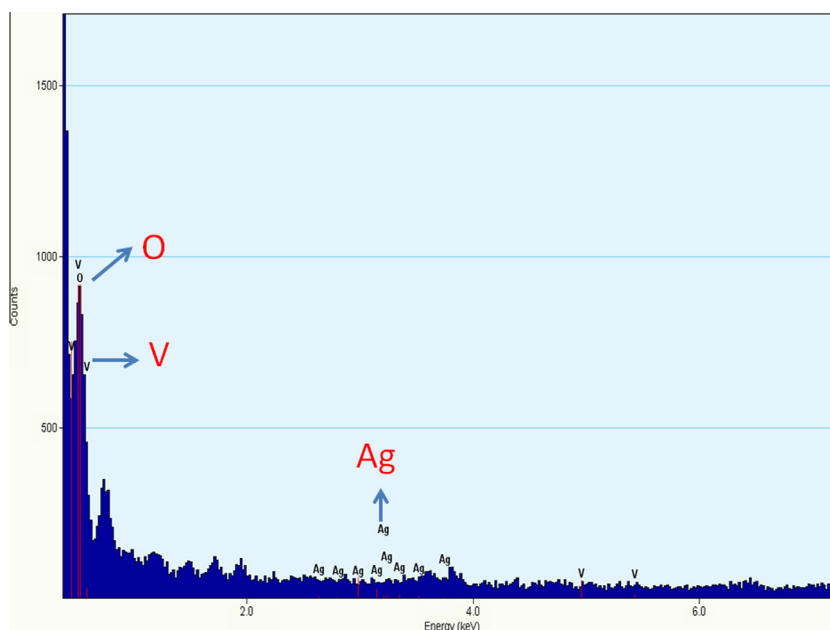


**Figure 6** EDX spectrum of  $\beta\text{-Ag}_{0.333}\text{V}_2\text{O}_5$  nanorods.



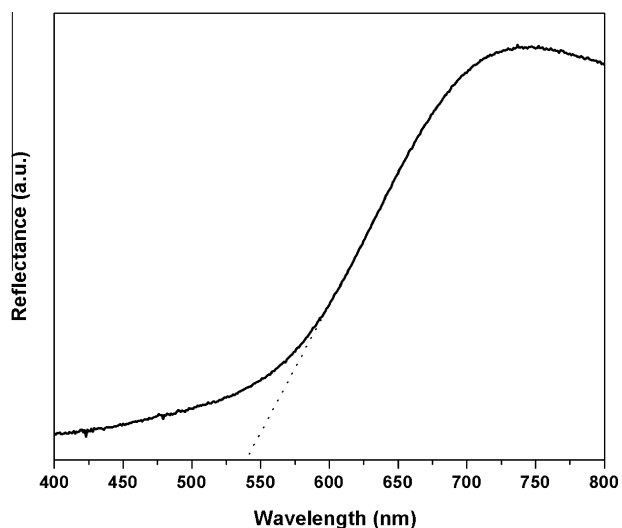


**Figure 7** Diffuse reflectance spectrum of  $\beta$ - $\text{Ag}_{0.333}\text{V}_2\text{O}_5$  sample.

### 3.1. Photocatalytic degradation of MO under visible light irradiation

The primary goal of this work is to degrade the organic pollutants using the prepared catalysts under visible light exposure.

For that purpose, MO was preferred as a model organic compound. The photocatalytic experiment was performed by the mineralization of MO aqueous solution in the presence of  $\text{Ag}_{0.333}\text{V}_2\text{O}_5$  catalysts under visible light illumination. At first, photosensitivity of the dyes was tested on blank MO aqueous solution without adding any catalysts under light illumination and later in the presence of catalyst under dark condition. As there was no change in MO concentration, these tests conclude that MO did not undergo any decomposition in both the cases mentioned earlier. Hence for the efficient degradation of MO aqueous solution, the presence of both catalyst and light is the necessary factor. Fig. 9 displays the change in absorption spectra of MO aqueous solution in the presence of  $\beta$ - $\text{Ag}_{0.333}\text{V}_2\text{O}_5$  catalysts as a function of visible light irradiation time. Fig. 8 reveals that the maximum absorption peak of MO at 464 nm decreases rapidly and completely decolorizes within 80 min in the presence of catalysts under visible light illumination. The photodegradation efficiency of  $\beta$ - $\text{Ag}_{0.333}\text{V}_2\text{O}_5$  catalysts was found to be 97% of MO in the visible light irradiation. Few researchers have used other compositions of SVO as a catalyst to eliminate the organic pollutants under visible light illumination [10–11,22–27]. In this present study,  $\beta$ - $\text{Ag}_{0.333}\text{V}_2\text{O}_5$  synthesized via thermal decomposition route shows the complete degradation of MO aqueous solution within 80 min than those reported in the previous literature studies [22–24,27]. The synthesis method, particle size and crystallinity of the catalyst were important factors which affect

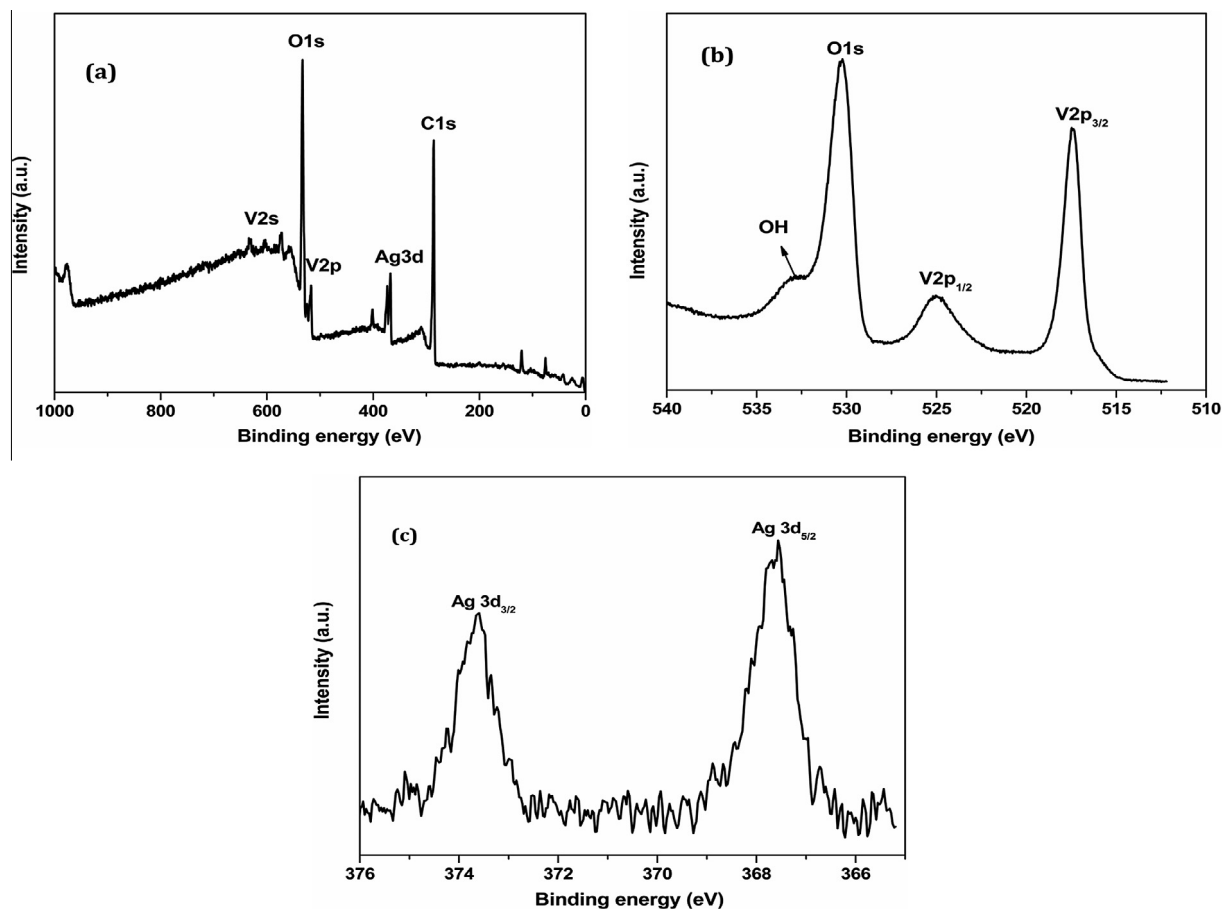


**Figure 8** XPS patterns of  $\beta$ - $\text{Ag}_{0.333}\text{V}_2\text{O}_5$  nanorods (a) survey spectrum, (b) high resolution spectrum of O 1s and V 2p and (c) high resolution spectrum of Ag 3d region.

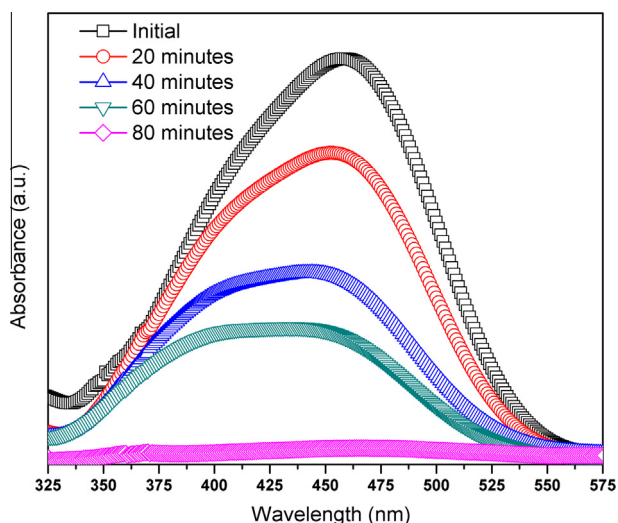


**Figure 9** UV-Vis absorption spectra of MO- $\beta$ - $\text{Ag}_{0.333}\text{V}_2\text{O}_5$  nanorods for uniform time intervals under visible light illumination.

the degradation time. The higher photocatalytic activity of  $\text{Ag}_{0.333}\text{V}_2\text{O}_5$  catalysts is due to the following two significant aspects: (1) The catalyst  $\beta$ - $\text{Ag}_{0.333}\text{V}_2\text{O}_5$  shows smaller particle size; when the particle size decreases, the surface area to volume ratio increases and thereby enhances the electron-hole separation. This results in the available active sites for surface reaction, thus leading to higher degradation efficiency of MO aqueous solution [28] and (2) Morphology of the catalysts plays an important role in enhancing the final degradation efficiency which had been reported in the literature [29]. The rod-shaped morphology more effectively degrades MB than other morphologies which have been reported by Kim et al. The higher activity of the rod shaped particles is due to its increased absorption property [30].

#### 4. Conclusion

In this report, one dimensional  $\text{Ag}_{0.333}\text{V}_2\text{O}_5$  nanorods have been successfully synthesized via facile thermal decomposition method without any additives. Degradation efficiency of  $\text{Ag}_{0.333}\text{V}_2\text{O}_5$  nanorods was achieved at 97% within 80 min. This outstanding photocatalytic activity is attributed to their smaller crystallite size and morphology. The results demonstrate that the facile thermal decomposition route is an efficient technique to synthesize the attractive morphology of the catalysts for promising applications in waste water treatment.

#### Acknowledgements

We acknowledge National Centre for Nanoscience and Nanotechnology, University of Madras, Chennai, India for XPS and TEM characterizations. The authors (R.S., F.G.) acknowledge the support of CONICYT through the project CONICYT/FONDAP/15110019 and the postdoctoral fellowship granted to R.S.

#### References

- [1] F.C. Wu, R.L. Tseng, High adsorption capacity NaOH-activated carbon for dye removal from aqueous solution, *J. Hazard. Mater.* 152 (2008) 1256–1267.
- [2] M.M. Khan, S.A. Ansari, M.I. Amal, J. Lee, M.H. Cho, Highly visible light active  $\text{Ag}@\text{TiO}_2$  nanocomposites synthesized using an electrochemically active biofilm: a novel biogenic approach, *Nanoscale* 5 (2013) 4427–4435.
- [3] A. Fujishima, T. N. Rao, Donald A. Tryk, Titanium dioxide photocatalysis, *J. Photochem. Photobiol. C: Photochem. Rev.* 1 (2000) 1–21.
- [4] M.M. Khan, J. Lee, M.H. Cho,  $\text{Au}@\text{TiO}_2$  nanocomposites for the catalytic degradation of methyl orange and methylene blue: An electron relay effect, *J. Ind. Eng. Chem.* 20 (2014) 1584–1590.
- [5] S.A. Ansari, M.M. Khan, M.O. Ansari, J. Lee, M.H. Cho, Biogenic synthesis, photocatalytic and photoelectrochemical performance of  $\text{Ag}-\text{ZnO}$  nanocomposite, *J. Phys. Chem. C* 117 (2013) 27023–27030.
- [6] R. Saravanan, V.K. Gupta, V. Narayanan, A. Stephen, Comparative study on photocatalytic activity of ZnO prepared by different methods, *J. Mol. Liquids.* 181 (2013) 133–141.
- [7] S. Kalathil, M.M. Khan, S.A. Ansari, J. Lee, M.H. Cho, Band gap narrowing of titanium dioxide ( $\text{TiO}_2$ ) nanocrystals by electrochemically active biofilms and their visible light activity, *Nanoscale* 5 (2013) 6323–6326.
- [8] M.M. Khan, S.A. Ansari, D. Pradhan, M.O. Ansari, D.H. Han, J. Lee, M.H. Cho, Band gap engineered  $\text{TiO}_2$  nanoparticles for visible light induced photoelectrochemical and photocatalytic studies, *J. Mater. Chem. A* 2 (2014) 637–644.
- [9] K.J. Takeuchi, A.C. Marschilok, S.M. Davis, R.A. Leising, E.S. Takeuchi, Silver vanadium oxides and related battery applications, *Coord. Chem. Rev.* 219 (2001) 283–310.
- [10] R. Konta, H. Kato, H. Kobayashi, A. Kudo, Photophysical properties and photocatalytic activities under visible light irradiation of silver vanadates, *Phys. Chem. Chem. Phys.* 5 (2003) 3061–3065.
- [11] G.T. Pan, M.H. Lai, R.C. Juang, T.W. Chung, T.C.K. Yang, Preparation of visible-light-driven silver vanadates by a microwave-assisted hydrothermal method for the photodegradation of volatile organic vapors, *Ind. Eng. Chem. Res.* 50 (2011) 2807–2814.
- [12] R.S. Devan, R.A. Patil, J.H. Lin, Y. Ron, Ma, One-dimensional metal-oxide nanostructures: recent developments in synthesis, characterization, and applications, *Adv. Funct. Mater.* 22 (2012) 3326–3370.
- [13] S. Liu, W. Wang, L. Zhou, L. Zhang, Silver vanadium oxides nanobelts and their chemical reduction to silver nanobelts, *J. Cryst. Growth* 293 (2006) 404–408.
- [14] H. Shi, Z. Li, J. Kou, J. Ye, Z. Zou, Facile synthesis of single-crystalline  $\text{Ag}_2\text{V}_4\text{O}_{11}$  nanotube material as a novel visible-light-sensitive photocatalyst, *J. Phys. Chem. C* 115 (2011) 145–151.
- [15] R. Saravanan, K. Santhi, N. Sivakumar, V. Narayanan, A. Stephen, Synthesis and characterization of ZnO and Ni doped ZnO nanorods by thermal decomposition method for spintronics application, *Mater. Charact.* 67 (2012) 10–16.
- [16] R. Saravanan, H. Shankar, T. Prakash, V. Narayanan, A. Stephen, ZnO/CdO composite nanorods for photocatalytic degradation of methylene blue under visible light, *Mater. Chem. Phys.* 125 (2011) 277–280.
- [17] Z.W. Pan, Z.R. Dai, Z.L. Wang, Nanobelts of semiconducting oxides, *Science* 291 (2001) 1947–1949.
- [18] M.M. Khan, S.A. Ansari, D. Pradhan, D.H. Han, J. Lee, M.H. Cho, Defect-induced band Gap narrowed  $\text{CeO}_2$  nanostructures for visible light activities, *Ind. Eng. Chem. Res.* 53 (2014) 9754–9763.

- [19] C.D. Wagner, W.M. Riggs, L.E. Davis, J.F. Moulder, G.E. Muilenberg, Handbook of X-ray Photoelectron Spectroscopy, Perkin-Elmer Corporation, Physical Electronics Division, USA, 1979.
- [20] V. Bondarenka, Z. Martunas, S. Kaciulis, L. Pandolfi, Sol-gel synthesis and XPS characterization of sodium-vanadium oxide bronze thin films, *J. Electron Spectrosc. Relat. Phenom.* 131 (2003) 99–103.
- [21] J.M. Song, Y.Z. Lin, H.B. Yao, F.J. Fan, X.G. Li, S.H. Yu, Superlong  $\beta$ -AgVO<sub>3</sub> nanoribbons: high-yield synthesis by a pyridine-assisted solution approach, their stability, electrical and electrochemical properties, *ACS Nano* 3 (2009) 653–660.
- [22] H. Lin, P.A. Maggard, Synthesis and structures of a new series of silver-vanadate hybrid solids and their optical and photocatalytic properties, *Inorg. Chem.* 47 (2008) 8044–8052.
- [23] J. Xu, C. Hua, Y. Xi, B. Wan, C. Zhang, Y. Zhang, Synthesis and visible light photocatalytic activity of  $\beta$ -AgVO<sub>3</sub> nanowires, *Solid State Sci.* 14 (2012) 535–539.
- [24] X. Hu, C. Hu, Preparation and visible-light photocatalytic activity of Ag<sub>3</sub>VO<sub>4</sub> powders, *J. Solid State Chem.* 180 (2007) 725–732.
- [25] C.M. Huang, G.T. Pan, Y.C.M. Li, M.H. Li, T.C.K. Yang, Crystalline phases and photocatalytic activities of hydrothermal synthesis Ag<sub>3</sub>VO<sub>4</sub> and Ag<sub>4</sub>V<sub>2</sub>O<sub>7</sub> under visible light irradiation, *Appl. Catal. A* 358 (2009) 164–172.
- [26] X. Hu, C. Hu, J. Qu, Photocatalytic oxidation of nitric oxide with immobilized titanium dioxide films synthesized by hydrothermal method, *J. Hazard. Mater.* 151 (2008) 17–25.
- [27] X. Hu, C. Hu, J. Qu, Preparation and visible-light activity of silver vanadate for the degradation of pollutants, *Mater. Res. Bull.* 43 (2008) 2986–2997.
- [28] R.M. Mohamed, D.L. McKinney, W.M. Sigmund, Enhanced nanocatalysts, *Mater. Sci. Eng., R* 73 (2012) 1–13.
- [29] L. Ren, L. Ma, L. Jin, J.B. Wang, M. Qiu, Y. Yu, Template-free synthesis of BiVO<sub>4</sub> nanostructures: II. Relationship between various microstructures for monoclinic BiVO<sub>4</sub> and their photocatalytic activity for the degradation of rhodamine B under visible light, *Nanotechnology* 20 (2009) 405602–405610.
- [30] S.J. Kim, D.W. Park, Preparation of ZnO nanopowders by thermal plasma and characterization of photo-catalytic property, *Appl. Surf. Sci.* 255 (2009) 5363–5367.